Original article

UDC 54.057, 54.058

DOI: 10.15372/CSD2025629

EDN: CLIHZY

Synthesis and application of nanocarbon materials for environmental purposes

Z. A. MANSUROV[1,2], M. A. SEITZHANOVA[2] ✉, S. AZAT[1,3]

[1]*Institute of Combustion Problems, Almaty, Kazakhstan*

[2]*Al-Farabi Kazakh National University, Almaty, Kazakhstan*

[3]*Satbayev University, Almaty, Kazakhstan*

E-mail: zmansurov@kaznu.kz, makpal_90.90@mail.ru✉, seytkhan.azat@gmail.com

Abstract

The results of studies conducted at the Institute of Combustion Problems (Almaty, Kazakhstan) on the synthesis of nanocarbon materials and their application for environmental purposes are presented. The procedures have been developed for obtaining nanocarbon materials from rice husk and walnut shells (graphenes and activated carbon, respectively), the physicochemical properties of the synthesised materials and the possibility of their practical use are studied. Graphene investigation by infrared and Raman spectroscopy allowed us to analyse the surface functional groups and the structural features of the material composed of a mixture of amorphous carbon and graphene, the ratio between these components depending on synthesis method. With an increase in the amount of the alkaline agent, the content of graphene component in the structure of carbon material increases. The porous structure and morphology of carbonised materials from rice husk and walnut shells were characterised according to the data of scanning electron microscopy. Nanocarbon graphene structures and activated carbon synthesised from the waste plant materials have demonstrated good adsorption properties for sea water desalination and sorption of toxic gases.

Keywords: carbon, nanomaterial, sorption, porosity, graphene

Funding: the studies on synthesis and application of carbon materials for purification from toxic gases were carried out with financial support from the Science for Peace and Security (SPS) NATO Programme under the project Valorisation of Biomass Waste into High Efficient Materials for Chemical, Biological, Nuclear, and Radiological Protection (Project Code G5636).

For citation: Mansurov Z. A., Seitzhanova M. A., Azat S., Synthesis and application of nanocarbon materials for environmental purposes, *Chemistry for Sustainable Development*, 2025, Vol. 33, No. 1, P. 43–52. DOI: 10.15372/CSD2025629. EDN: CLIHZY.

INTRODUCTION

Carbon nanomaterials include nanostructured carbon substances composed mainly of carbon, with particle/pore size of less than 100 nm. The application of carbon nanomaterials for environmental purposes requires focused attention because they can be efficient in solving many problems associated with environmental pollution and climate change. In the present work, two kinds of nanostructured materials synthesised from waste plant materials (rice husk and walnut shells) are

presented, along with the possible ways of their application: water desalination and adsorption-based air purification.

Graphene is an allotropic modification of carbon, comprising flat two-dimensional layers of regular hexagons composed of carbon atoms in the sp^2-hybrid state. Graphene is schematically represented as a sheet of hexagonal honeycombs with a thickness of a single carbon atom, and it is considered as one of the most promising materials discovered recently. From the viewpoint of practical use, graphene is relevant for multifunctional purposes, from power engineering and environmental protection to health services [1–3]. At present, new methods of obtaining graphene are emerging with the use of non-traditional and cheap precursors. Renewable and stable resources in the form of biomass are considered as the reasonable versions of raw materials to obtain a graphene precursor. The approaches of this kind for obtaining graphene materials from rice husk (RH) have been recently considered in [4]. Rice husk is the shells of rice grains, and this is one of the best available agricultural wastes in many rice manufacturing countries. The use of RH directly for the production and synthesis of materials with added value is a feasible strategy for solving the problem of waste utilisation and reduction of expenses for waste recycling [5].

Another valuable carbon-containing precursor can be walnut shells (N). This kind of plant raw materials is characterised by the high content of carbon component and very small amount of ash substances, which is a favourable factor for processing this kind of raw material into carbon sorbents, because it allows a reduction of the expenses for the recovery of minerals from the final product. Walnut shells are one of the most promising plant raw materials to produce activated coal for use in the food industry and in medicine. Activated coal obtained from the indicated plant raw material is characterised by high specific surface area and highly developed porous structure, so it is considered to be one of the most promising industrial adsorbents [6].

It is still urgent to develop the optical parameters of the technology for obtaining carbon materials from the indicated kinds of natural raw material, to study the features of their structure, surface properties and morphology, and to investigate the relationship between these properties and the practical potential of final products.

The goal of the present work was to use the available plant raw material (rice husk and walnut shells) to synthesise graphene and activated coal, respectively, to study the morphological and physicochemical properties of the samples, and to investigate the potential of the application of synthesised nanocarbon materials as porous membranes for water desalination and filters for air purification from toxic gases.

EXPERIMENTAL

Materials

The materials used to synthesise graphene and to manufacture membranes included rice husk, sodium hydroxide, potassium hydroxide, hydrogen peroxide, polyethylene imine (PEI), *N*-methyl-2-pyrrolidone, polyvinyl pyrrolidone (PVP).

To synthesise activated coal, the following materials and reagents were used: walnut shells, 70 % phosphoric acid, distilled water.

To prepare gas filters, activated coal was impregnated with the solutions of copper, cobalt and nickel nitrates.

Desalinating ability of membranes was tested for the solutions of salts: NaCl, KCl, $MgCl_2$, $CaSO_4$ and $MgSO_4$.

Methods of investigation

Investigation of the functional groups on the surface of materials was carried out by IR spectroscopy (0.5–0.8 wt% in KBr) using a Nicolet 5700 spectrometer (Thermo Electron, USA) within a wavenumber range of 3600–400 cm^{-1}.

The images of local sites of the surface were taken by scanning electron microscopy (SEM) using a scanning microscope FEI Inspect™ S50 (Thermo Fisher Scientific, USA) with the low vacuum mode for industrial applications with the possibility to reach high resolution when the thermoemission electron optics is used.

The structure of carbon nanomaterials was studied by Raman spectroscopy. The spectra were recorded with a Raman microscope NRS-3100 (Jasco, USA). The line of Ar^+ water-cooled laser at the wavelength of 514 nm, with a power of 4 MW directed at the sample, was introduced into the embedded microscope Olympus and focused on a spot about 2 μm in diameter with the help of a 100× objective. To suppress the laser excitation line, a holographic band-refection filter was used. The Raman spectra were recorded with a cooled CCD photon detected with the resolution

of 1024 × 128 pixels (Andor DU401BVI). To provide reproducibility, Raman spectra were recorded at least three times. Hexane was used for calibration.

The composition of solutions filtered through the membranes was studied with the atomic absorption flame-ionisation spectrophotometer AA-6200 (Shimadzu, Japan) at the Centre for Physicochemical Studies and Analysis (Almaty, Kazakhstan) employing the following discretisation modes: a dual-beam optical system, a Czerny–Turner monochromator, 190–900 nm spectral range, 0.2, 0.7 nm spectral sampling interval (switched manually), deuterium as a background corrector, simultaneous switching on (one is working, the other is heating).

RESULTS AND DISCUSSION

Graphene synthesis

Carbon-containing materials composed of graphene layers were obtained from rice husk (RH) using the top-down method, by following a four-stage strategy: preliminary carbonisation, desilication, chemical activation, and exfoliation. At first, RH was washed with distilled water several times to remove impurities, and then dried at a temperature of 383 K for 1 h. After that, RH was carbonised preliminarily for 45 min in a rotating reactor in the atmosphere of argon at a temperature within the range of 523–573 K and a gas flow rate of 5 cm^3/min. Thus obtained preliminarily carbonised material obtained from rice husk (CRH) was desilicated by treating 60 g of CRH with a 1 M NaOH solution in the amount of 3 L at 353 K for 3 h. The suspension was separated from the solution by decanting, washed to the neutral pH, and dried in the furnace (383 K, 2 h). To activate desilicated sample, it was mixed with ground KOH varying the carbon to KOH ratio (1 : 4 and 1 : 5). The mixtures were compacted in an iron crucible and annealed at 1123 K for 2 h in the atmosphere of Ar. After activation treatment, the resulting samples marked as Gr(1/4) and Gr(1/5), respectively, were washed with distilled water to neutral pH and dried at 373 K for 24 h. The sample Gr(1/4) was subjected to exfoliation to remove amorphous carbon by treating the material with a 37 vol% H_2O_2 solution for 48 h, after which it was washed and dried. Product yield was ~3 wt% of the total mass of RH and potassium hydroxide [7–9].

Manufacturing the graphene-containing membrane

Membranes made of carbon modified with polyethylene imine (PEI) were obtained by immersion deposition, referred to as the nonsolvent induced phase separation (NIPS) technology. Carbon black was also used as a carbon model for comparison. At first, 0.41 g of PEI and 1.95 mL of N-methyl-2-pyrrolidone (NMP) were added into the flask, and heated at a temperature about 323 K at mixing for 18 h to obtain a homogeneous solution of the polymer. Then 0.1 g of graphene sample (Gr(1/4) or Gr(1/5)) was dispersed in a small amount of NMP (1 mL), treated with ultrasound for 30 min, and then PEI was added to the suspension. After that, 0.1 g of polyvinyl pyrrolidone (PVP) was added to the dispersed suspension (PEI – graphene) and carefully mixed for 1 h to obtain a uniform suspension. Thus obtained suspension was degassed with ultrasound to remove the captured air bubbles. The homogeneous solution for moulding was poured along a glass plate, bringing the layer thickness to 400 μm, and immersed for coagulation into a bath filled with water. Thus obtained membrane was kept in the coagulation bath for 24 h to provide total inversion of the phases.

Investigation of the synthesised graphenes

The results of elemental analysis are graphically presented in Fig. 1, *a*. Carbonisation of RH at 1123 K in combination with chemical activation (Gr(1/4) sample) is seen to cause an increase in carbon content to ~75 wt% in comparison with the product of carbonisation without alkaline activation (CRH sample) containing ~55 wt% carbon, in addition, the sample Gr(1/4) is characterised by lower hydrogen concentration. This feature was also revealed with the help of IR spectroscopy (see Fig. 1, *b*). The spectrum of CRH is characterised by a set of signals related to different functional groups: low-intensity absorption bands (a. b.) around 3000 cm^{-1} are due to the stretching vibrations of aliphatic and aromatic C–H bonds, while in the medium-frequency range (1700 and 1000 cm^{-1}) a broad set of peaks is observed, related to overlapping of the a. b. of carbon framework (the stretching and bending modes of C=O, C=C, C–C, C–H, C–O bonds). These features were described in [7, 8]. The spectra of Gr(1/4) and Gr(1/5) are represented by a broad band characteristic of large condensed aromatic networks. These spectra contain not only

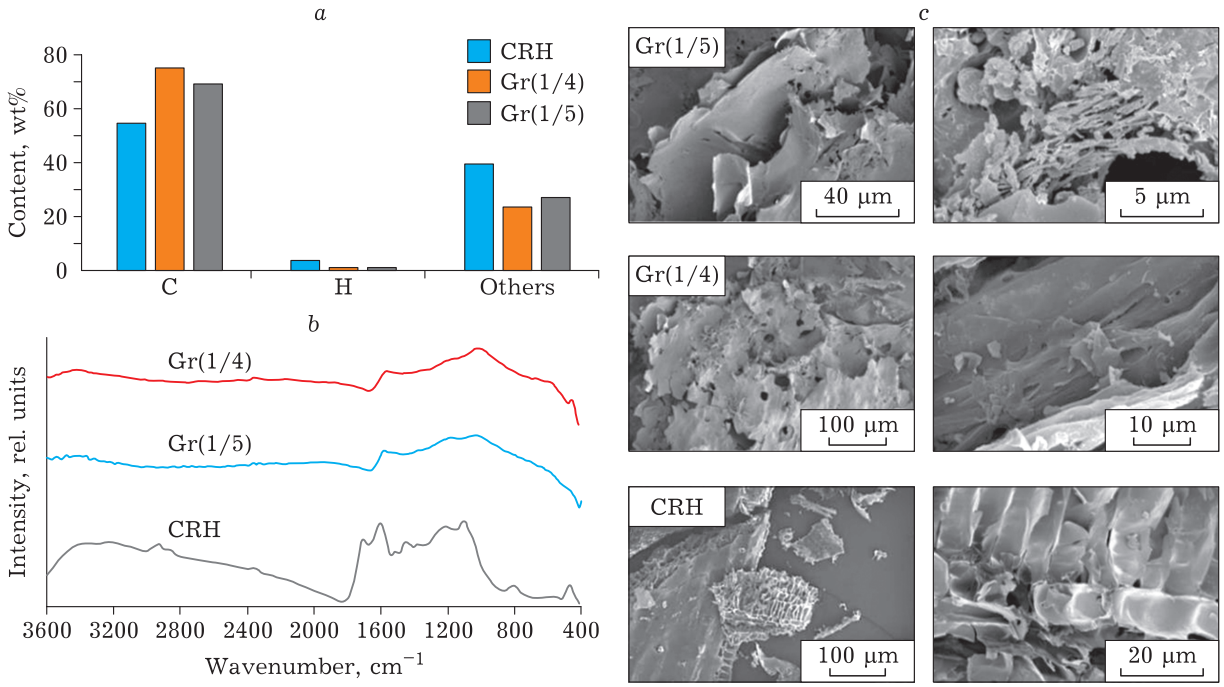

Fig. 1. The data of elemental analysis (*a*), IR spectra (*b*) and SEM images at different magnification (*c*) of the rice husk samples after carbonisation (CRH) and subsequent alkaline activation with different CRH/KOH ratios (samples Gr(1/4) and Gr(1/5)).

a. b. related to C=C stretching modes but also the bands overlapping within the range from 900 to 1500 cm^{-1}, related to the vibrations of the framework. For the dispersions of solid samples prepared for examination by IR spectroscopy, the direct current conductance (σ) was measured to be, nS/m: 14±3 for CRH, 80±10 for Gr(1/4), and 60±10 for Gr(1/5). The observed trend to increasing σ values for the alkaline-activated materials provides evidence that a longer conducting part was achieved in graphene samples (Gr(1/4) and Gr(1/5)).

SEM images of CRH, Gr(1/4) and Gr(1/5) at different magnifications (see Fig. 1, *c*) provide evidence that CRH is a highly porous material with the large internal surface area. The morphology of carbonised product (CRH) exhibits no substantial differences in co0mparison with raw rice husk. The samples Gr(1/4) and Gr(1/5) have a layered structure with the wrinkled silk veil effect and noticeable folded regions. In general, after activation the sample morphology appears to be more definite and ordered (see Fig. 1, *c*, right): graphene sheets form a layer-by-layer structure over the whole cross section, broadening permanently in the longitudinal direction. However, micrometre-sized cavities are formed between graphene layers during annealing, which leads to higher porosity.

The Raman spectra demonstrate specific features of the CRH sample: the presence of D and G bands, related to amorphous carbon, the absence of G′ band (also called 2D) at about 2700 cm^{-1}, which is characteristic of non-amorphous sp2-carbon structures. The Raman spectra of samples Gr(1/5) and Gr(1/4), shown in Fig. 2, unambiguously point to a mixture of the amorphous and graphene components. Substantial spatial inhomogeneity has been discovered, but two major components can be distinguished: amorphous carbon with D and G bands at 1352 and 1594 cm^{-1}, respectively, and graphene with characteristic bands D, G and G′.

The Raman spectra were recorded for different regions (points) of samples Gr(1/5) and Gr(1/4), differing by their morphology (bands *1*–*4*, see Fig. 2). The ratios of the integral intensities of G and G′ bands (I_G/I_G') were analysed only for amorphous regions (see Fig. 2, bands *1*, *3*, *4*), because this ratio for graphene was determined to be insignificant (marked with a star on band *2*). For both samples Gr(1/5) and Gr(1/4), the ratio I_G/I_G' is close to 1.56±0.10, which is evidence of the multi-layered structure. Comparing samples Gr(1/4) and Gr(1/5) within a limited set, we determine that the ratio CRH/KOH at activation, equal to 1 : 5, provides a higher graphene content than 1 : 4 does.

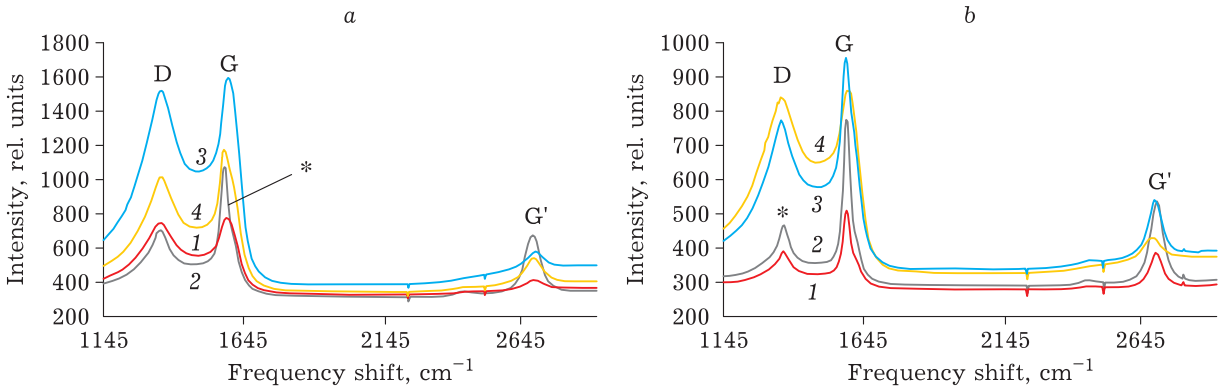

Fig. 2. Raman spectra of the samples Gr(1/4) (*a*) and Gr(1/5) (*b*). Bands (*1–4*) correspond to different local regions (points) of the samples differing from each other in morphology.

Investigation of the characteristics of resulting membranes

The composition and thickness of membranes (M) made of PEI-modified carbon are presented in Table 1.

Changes in the morphology of PEI membrane cross section after the addition of modified graphene (washed and functionalised) and carbon black into the membrane matrix were analysed by SEM. Before SEM analysis, the cry membrane was subjected to cryogenic destruction, and a thin gold layer was applied using a spraying device.

The SEM images of the cross section of the nanocomposite membrane matrix with different amounts of additive are presented in Fig. 3. All membranes had asymmetric structure with a dense upper layer, followed by a porous sublayer with well-developed macropores, which is a typical morphological pattern of the membranes manufactured by phase inversion.

The desalinating properties of membranes were studied in the experiments on salt removal from five salt-containing liquids at room temperature using a usual filtration system (Fig. 4). The initial solution was poured into the mixing cell (*1*) with the effective membrane area of 38 mm^2 (*3*) and the receiver reservoir of 300 mL in volume (*5*). The total volume of the initial solution was 200 mL, taking into account the volumes of mixing cell and the solution feed vessel. Filtration pressure was provided and regulated with a pump. The manufactured membranes were used for each filtration test. A stable flow of distilled water was measured and compared between different membrane samples to check the reproducibility of the filtering ability of the synthesised membranes.

Desalinating properties of the membranes were tested for NaCl, KCl, $MgCl_2$, $CaSO_4$ and $MgSO_4$. Salt concentrations were determined using an atomic absorption flame emission spectrophotometer. The results of the experiment are shown in Fig. 5. The initial salt concentration was, g/L: NaCl 27.300, KCl 0.700, $MgCl_2$ 2.275, $CaSO_4$ 1.225, $MgSO_4$ 2.275. After filtration, salt concentration decreases to, g/L: NaCl 1.647, KCl 0.189, $MgCl_2$ 0.199, $CaSO_4$ 0.183, $MgSO_4$ 0.267.

The mechanisms of water filtration through a graphene membrane are related to the unique properties of graphene, including its ultrafine

TABLE 1

Composition and thickness of the synthesised membranes

Sample	NMP, mL	PEI, g	PVP, g	Gr(1/4), g	Gr(1/5), g	CB, g	Thickness, μm
M PVP/PEI	1.95	0.41	0.1	–	–	–	150
M PVP/PEI/Gr(1/4)	1.95	0.41	0.1	0.1	–	–	360
M PVP/PEI/Gr(1/5)	1.95	0.41	0.1	–	0.1	–	270
M PVP/PEI/CB	1.95	0.41	0.1	–	–	0.1	370

Notes. 1. M – membrane; PEI – polyethylene imine; PVP – polyvinyl pyrrolidone; NMP – N-methyl-2-pyrrolidone; Gr(1/4) and Gr(1/5) – the products of rice husk carbonisation after alkaline activation at different ratio of the carbonisate (CRH) to KOH, equal to 1 : 4 and 1 : 5, respectively; CB – carbon black. 2. Dash – a component is not included in the formulation.

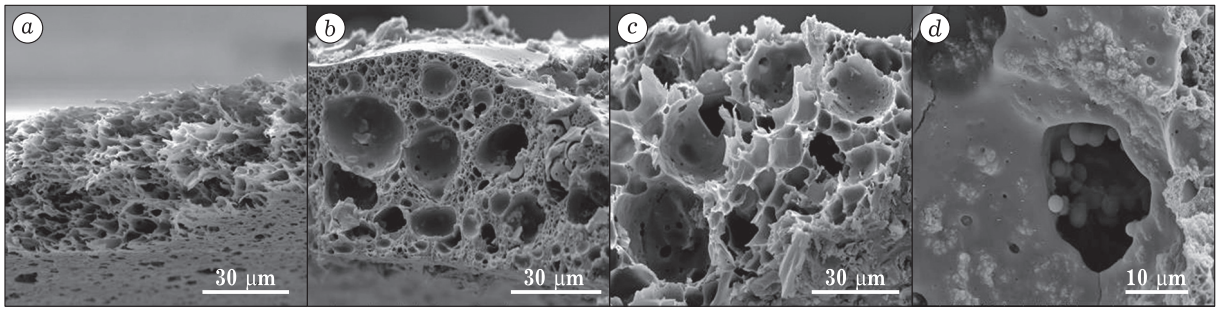

Fig. 3. SEM images of the samples of membranes (M) based on polyethylene imine (PEI), polyvinyl pyrrolidone (PVP), the products of rice husk carbonisation after alkaline activation (Gr(1/4) and Gr(1/5)), and carbon black (CB): M PVP/PEI (*a*), M PVP/PEI/Gr(1/4) (*b*), M PVP/PEI/Gr(1/5) (*c*), and M PVP/PEI/CB (*d*).

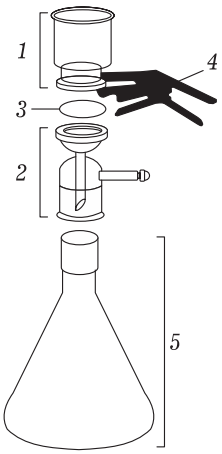

Fig. 4. Laboratory vacuum filtering apparatus: *1* – filtering beaker 300 mL in volume; *2* – filtering head; *3* – filtering membrane; *4* – clamp; *5* – conical flask 500 mL in volume.

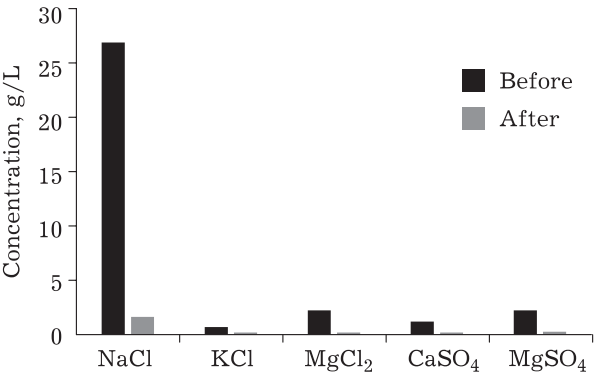

Fig. 5. Salt concentration before and after filtration.

structure, chemical modification, and hydrophobicity. Two types of graphene membranes and the mechanisms of water and salt ion transport through them are presented in Fig. 6:

1. Nanoporous graphene membrane. Only water molecules can pass through the nanopores, while larger molecules are retained by the filter. The additional filtering effect is promoted by ion repulsion or attraction, depending on the membrane charge. This membrane is composed of one graphene layer with nanopores, which provides a high filtration rate.

2. Layered membrane made of graphene oxide (GO). Filtration takes place due to narrow channels between GO layers through which only water molecules pass. Salt ions (with the size: Na^+ ~0.716 nm, K^+ ~0.662 nm, Cl^- ~0.664 nm, Mg^{2+} ~0.856 nm, Ca^{2+} ~0.823 nm) are held due to electrostatic binding, the interactions of a cation with π-bonds in graphene structure, and coordination with metals. Similarly to the former case, the interactions between membrane and ion charges regulate the motion of molecules. The membrane is composed of several GO layers, forming a layered structure with nanochannels. This enhances the selectivity and efficiency of filtration.

To put it with more clarity, a π-bond is the type of chemical bonds between carbon atoms in the structure of graphene, as well as other organic molecules in which carbon atoms form double or triple bonds. Carbon atoms are bound in graphene through π-bonds along the plane of the structure, which renders unique properties to graphene: high conductivity and the ability to interact with ions. In the case of the membrane made of graphene oxide (GO), metal ions can interact with the electron clouds of these π-bonds, which promotes retention of salt ions due to the interactions of cations with π-bonds.

According to the types of membranes, six key mechanisms can be distinguished [10], providing salt retention (preventing salt molecules or admixtures from passing through) by the multilayer graphene membranes:

1. Withdrawal by size. The membranes possess a porous structure with the pores smaller than the diameter of hydrated ions. This allows efficient retention of large ions and molecules, so

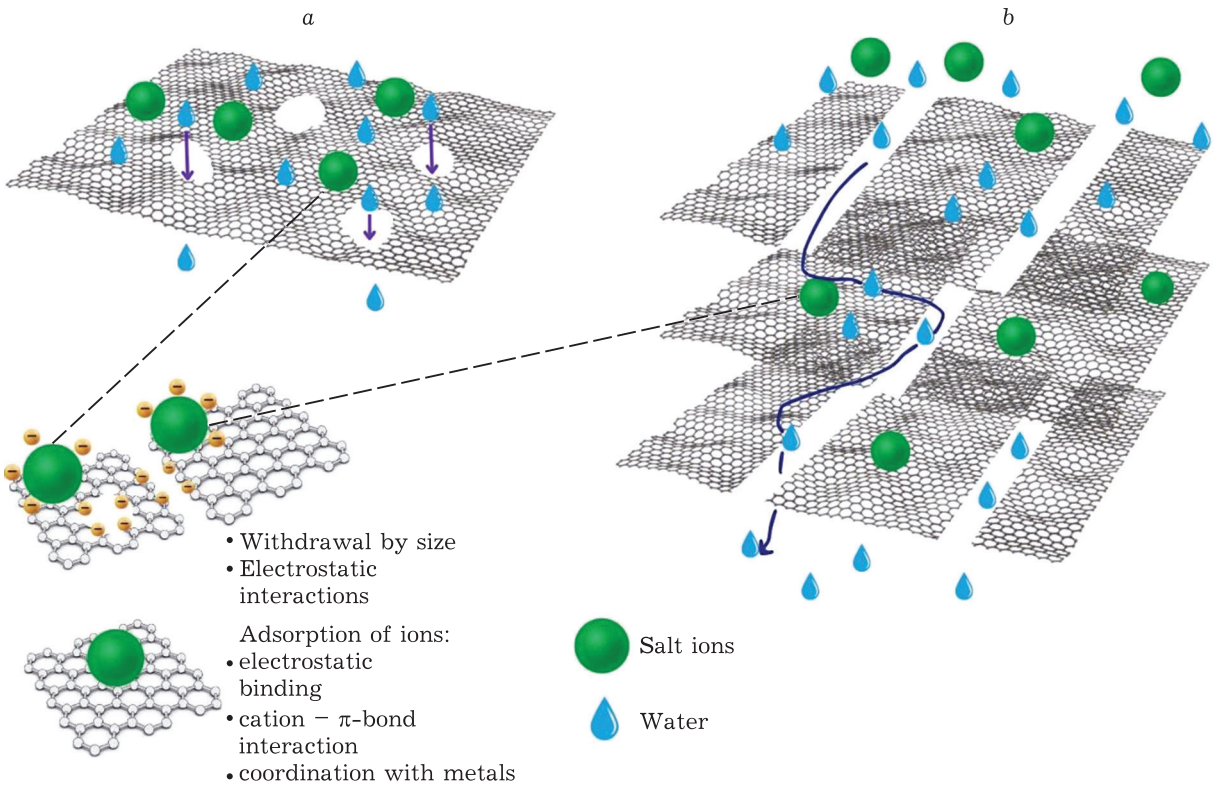

Fig. 6. Schematic separation mechanisms for a one-layer graphene membrane with the nanopores of controlled size (*a*) and a multilayer graphene membrane (*b*) composed of the folded sheets of graphene oxide (GO).

that only water molecules pass through because their diameter is smaller (~0.275 nm).

2. Dehydration. To pass through nanopores, the ions have to lose their hydration shells completely or in part, which will allow excluding the steric (geometric) effects. However, since there are no energy-related prerequisites for dehydration, the hydrated ions with large diameters are retained at the inlet of pores in the membrane.

3. Charge repulsion. The surface of graphene membranes often bears a charge (for example, because of the presence of functional groups in graphene oxides), which forms an electrostatic field. This field prevents the penetration of similarly charged ions, thus enhancing the selectivity of the membrane.

4. Specific interactions with pores. Like biological channels, some pores can interact with definite molecules or ions due to the chemical nature of their internal surface. These may be the interactions of the type of an ion − π-bond, hydrogen bonds or coordination bonds with metals (Na, K, Mg).

5. Chemical selectivity of the pores. Dissolved substances, such as salts, can interact with the functional groups inside the pores (for example, with carboxyl or hydroxyl groups), which additionally prevents their penetration through the membrane.

6. Entropy differences. The differences in the entropy properties of water and ions during their passing through nanopores play an essential part. The ions tend to stay in more stable hydrated states, while the restrictions created by the porous structure cause a decrease in their entropy, thus preventing percolation.

These mechanisms work together, providing the high selectivity of graphene membranes in separating salts and other impurities. For instance, a decrease in pore size enhances the effects of prevention salt molecules from passing through because of their size and dehydration, while the chemical modification of membrane surface improves its ability to repel or capture specific ions. Together, these processes confirm the potential of multilayer graphene membranes for water desalination and other tasks related to filtration.

Synthesis and application of carbon materials for purification from toxic gases

In the present work, the samples of activated coal obtained from walnut shells (N) were modified by copper, cobalt and nickel nitrates for use

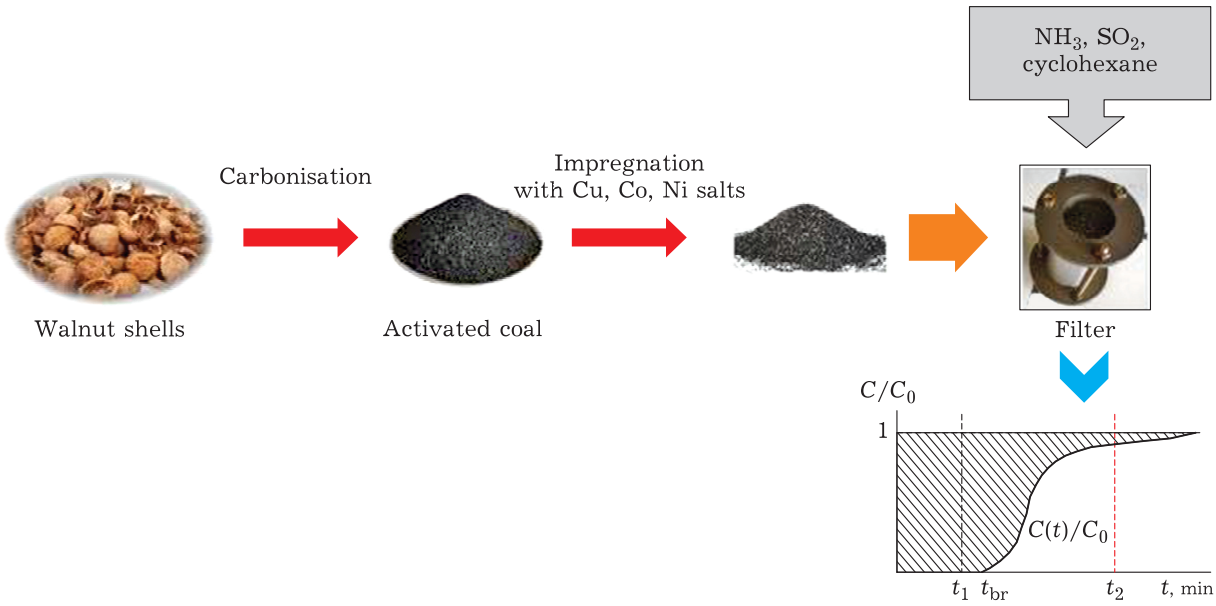

Fig. 7. Processing biomass wastes into highly efficient reactive sorbents for air purification from toxic gases. The plot shows the efficiency of purification at different stages of the adsorption of toxic gases (for example, NH_3, SO_2 or cyclohexane vapour): C_0, C – the concentration of the substance to be adsorbed, before and after filtration through the sorbent, respectively, t_{br} – breakthrough time.

in gas filters. This approach is aimed at processing the biomass wastes into highly efficient reactive sorbents against toxic gas emissions [11, 12] (Fig. 7).

Walnut shells were used as the raw material. This plant material is characterised by the low sulphur, nitrogen and ash content, as well as high carbon content. Walnut shells were ground and sieved to obtain the working fraction with particle diameters within the range of 2–4 mm. This fraction was washed with distilled water several times, and dried at room temperature for 6–12 h. The samples were chemically activated with 70 % phosphoric acid. At heating, phosphoric acid forms a protective film on particle surface. The film is composed of polyphosphoric acid and phosphorus polyoxides. It prevents combustion from the surface of the material without the formation of a developed porous structure of activated coal. In addition, phosphoric acid is an activating agent, similar to atmospheric oxygen and water vapour, which are released during carbonisation simultaneously providing activation. At first, the sample was impregnated with 70 % sulphuric acid and thermostated at 323 K for 12 h. The sample mass for the experiment was 50 g. The resulting dark-brown mixture was carbonised under isothermal conditions under strict control using a rotating reactor in the atmosphere of inert gas (argon), permanently supplied at a flow rate of 50 cm^3/min. The product was subjected to carbonisation at 1023±50 K. The rate of temperature rise was set with a VARTA temperature regulator (Germany) at 10 K/min. Carbonisation time was 90 min. After carbonisation, it is important to wait for the temperature to decrease to 473 K. The chemically activated sample was then washed with distilled water to pH 7 to remove residual phosphoric acid. After that, the sample was placed in the microwave furnace at 383 K and dried for 12 h. The samples were impregnated with the solutions of copper, cobalt and nickel nitrates by treating in the ultrasonic bath for 2 h and subsequent purification by washing with distilled water to reach the neutral pH value.

Analysis of the microstructure of carbon material samples shows (Fig. 8 and 9) that the activation method employed promotes the formation of a large number of fine pores and the development of the porous structure of sorbents. The activated samples are characterised by the large micropore volume and pronounced mesoporosity, which is confirmed by the corresponding isotherms of low-temperature nitrogen adsorption and the curves of pore size distribution (Fig. 10). In addition, it has been demonstrated that the samples with different acidity were formed after activation, and this feature of the surface has a substantial effect on the characteristics of the materials [13, 14].

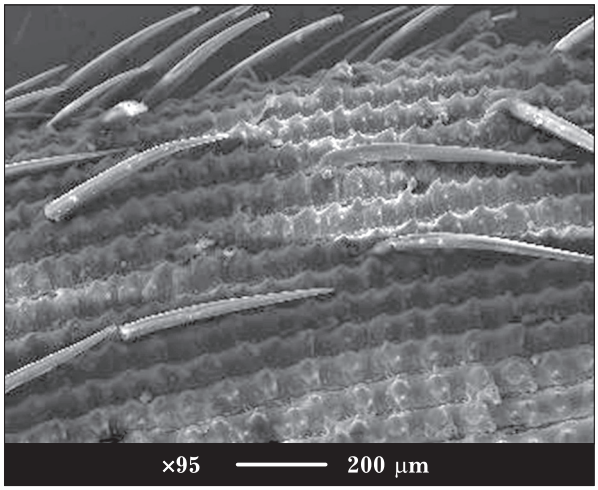

Fig. 8. Micrograph of walnut shell surface.

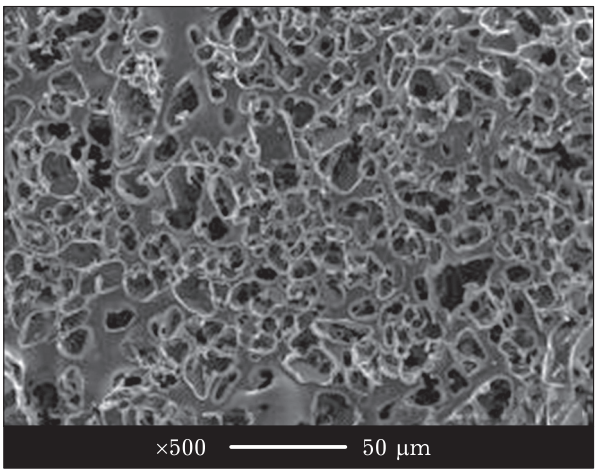

Fig. 9. Micrograph of the surface of carbon material prepared from walnut shells.

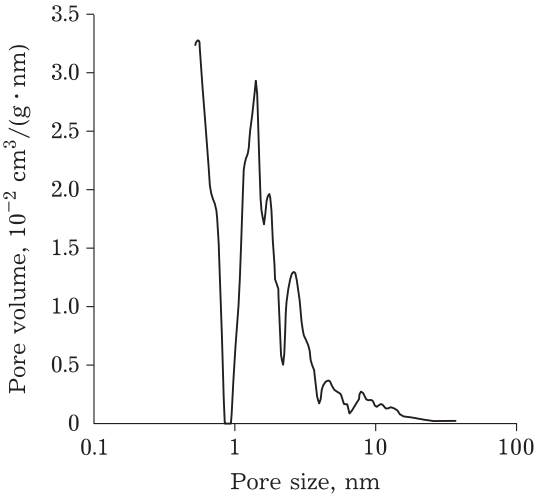

Fig. 10. Differential pore volume distribution in the sample of carbon material prepared from walnut shells.

Then different metal salts were used to obtain a series of impregnated activated coal samples. The efficiency of these materials with respect to the removal of organic vapours and mixtures (cyclohexane, cyclohexane + 1,2-dichloroethane), as well as inorganic gases (SO_2, NH_3), was assessed relying on the experimental breakthrough time values (t_{br}), determined using a special test installation. In this connection, especially promising results for the sorption of organic vapours and inorganic gases were obtained with nanocarbon based on walnut shells, saturated with cobalt: NCo sample (Fig. 11). These results demonstrate the high potential of these materials in the area of air purification, which opens the possibilities of their further application and development of more efficient sorption technologies. Special attention should be paid to nanocarbon materials because they have demonstrated substantial advantages in efficiency over traditional sorbents.

CONCLUSION

Graphene membranes prepared from carbonised rice husk by immersion deposition (NIPS technology) have demonstrated high efficiency of salt filtration. Carbonisation/activation of rice husk leads to the formation of a mixture of graphene layers and amorphous carbon. Larger amount of the activating agent (the ratio carbon/KOH = 1 : 5) is likely to cause an increase in the relative amount of the graphene component, while the number of layers remains the same. Sample exfoliation by hydrogen peroxide appeared to have a negative effect on graphene content and caused its layering from amorphous carbon. The results of SEM studies show that graphene membranes ~200 μm thick have a developed macroporous structure with the pores ~10 μm in size. Desalinating capacity of graphene membranes was tested with NaCl, KCl, $MgCl_2$, $CaSO_4$ and $MgSO_4$. The results show that the concentrations of these salts decreased by 70–95 % after filtration.

Activated coals modified with metals (Cu, Co and Ni) were obtained from walnut husk. It has been determined that activation results in obtaining nanosorbents with different acidity, and they are characterised by a large number of fine pores and developed porous texture. This approach is aimed at processing biomass wastes into highly

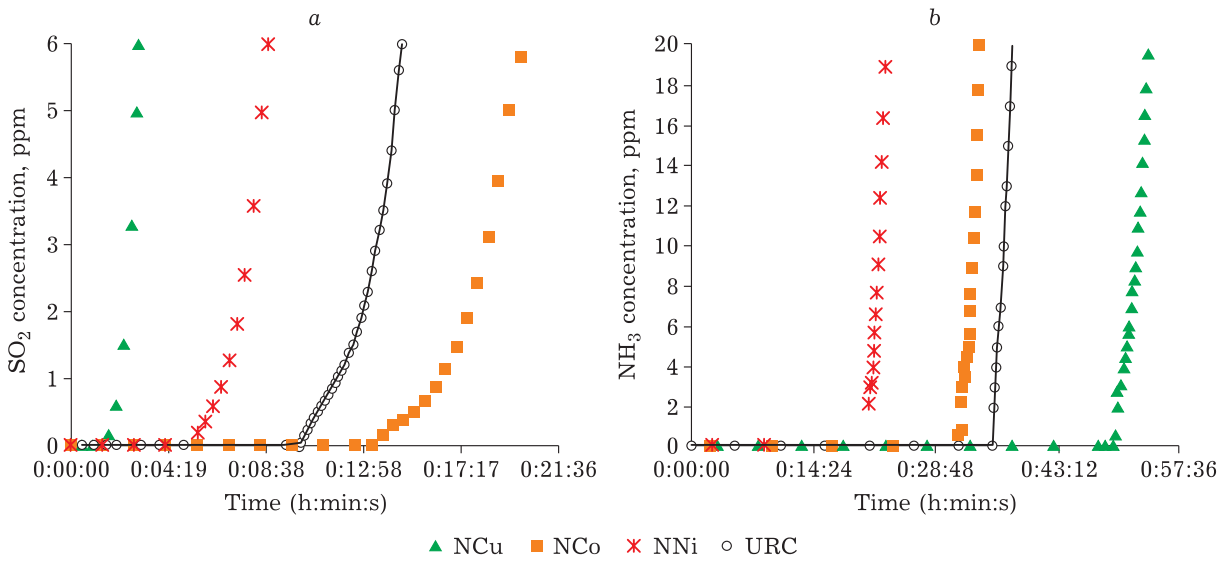

Fig. 11. Experimental curves of breakthrough time for SO_2 (*a*) and NH_3 (*b*) through carbon sorbents NCu, NCo, NNi (activated coal impregnated with copper, cobalt and nickel nitrates, respectively) and commercial sorbent URC.

efficient reactive sorbents to purify air from the emissions of highly toxic gases.

REFERENCES

1. Mansurov Z. A., Soot Formation, Kazakh University, Almaty, 2015, 167 p.
2. Ren S., Rong P., Yu Q., Preparations, properties and applications of graphene in functional devices: a concise review, *Ceram. Int.*, 2018, Vol. 44, No. 11, P. 11940–11955.
3. Alfè M., Gargiulo V., Di Capua R., Chiarella F., Rouzaud J.-N., Vergara A., Ciajolo A., Wet chemical method for making graphene-like films from carbon black, *ACS Appl. Mater. Interfaces*, 2012, Vol. 4, No. 9, P. 4491–4498.
4. Sankar S., Lee H., Jung H., Kim A., Ahmed A. T. A., Inamdar A. I., Kim H., Lee S., Im H., Kim D. Y., Ultrathin graphene nanosheets derived from rice husks for sustainable supercapacitor electrodes, *New J. Chem.*, 2017, Vol. 41, No. 22, P. 13792–13797.
5. Seytzhanova M. A., Kerimkulova M. R., Shyntoreev E. B., Azat S., Kerimkulova A. R., Mansurov Z. A., Development of the method for obtaining carbon ceramic adsorbents based on porous carbon, *Chemical Bulletin of Kazakh National University*, 2015, No. 2 (78), P. 37–41. (In Russ.).
6. Azat S., Busquets R., Pavlenko V. V., Kerimkulova A. R., Whitby R. L. D., Mansurov Z. A. Applications of activated carbon sorbents based on Greek walnut, *Applied Mechanics and Materials*, 2014, Vol. 467, P. 49–51.
7. Seitzhanova M. A., Chenchik D. I., Yeleuov M. A., Mansurov Z. A., Capua R. D., Elibaeva N. S., Synthesis and characterization of graphene layers from rice husks, *Chemical Bulletin of Kazakh National University*, 2018, Vol. 89, No. 2, P. 12–18.
8. Seitzhanova M. A., Yashnik S. A., Ismagilov Z. R., Khairulin S. R., Mansurov Z. A., Montaeva A. A., Investigation of the nature of functional groups of graphene membranes by means of IR spectroscopy, *Chem. Sustain. Dev.*, 2020, Vol. 28, No. 5, P. 480–486.
9. Jandosov J. M., Shikina N. V., Bijsenbayev M. A., Shamalov M. E., Ismagilov Z. R., Mansurov Z. A., Evaluation of synthetic conditions for H_3PO_4 chemically activated rice husk and preparation of honeycomb monoliths, *Eurasian Chem. Technol. J.*, 2009, Vol. 11, No. 3, P. 245–252.
10. Thomas M., Corry B., Hilder T. A., What have we learnt about the mechanisms of rapid water transport, ion rejection and selectivity in nanopores from molecular simulation?, *Small*, 2014, Vol. 10, No. 8, P. 1453–1465.
11. Hebbar R. S., Isloor A. M., Prabhu B., Inamuddin, Asiri A. M., Ismail A. F., Removal of metal ions and humic acids through polyetherimide membrane with grafted bentonite clay, *Sci. Rep.*, 2018, Vol. 8, Art. 4665.
12. Mansurov Z. A., Velasco L. F., Lodewyckx P., Doszhanov E. O., Azat S., Modified carbon sorbents based on walnut shell for sorption of toxic gases, *J. Eng. Phys. Thermophys.*, 2022, Vol. 95, No. 6, P. 1383–1392.
13. Mansurov Z. A., Doszhanov E. O., Lodewyckx P., Velasco L. F., Boutillara Y., Azat S., Synthesis and Application of Carbon Materials for Purification from Toxic Gases, Daryn, Almaty, 2022, 223 p. (In Russ.).
14. Mansurov Z. A., Lodewyckx P., Velasco L. F., Azat S., Kerimkulova A. R., Modified sorbents based on walnut shell for sorption of toxic gases, *Mater. Today Proc.*, 2022, Vol. 49, No. 6, P. 2521–2526.

Submitted 03.09.2023
Approved 01.06.2024
Accepted 12.07.2024